Journal of Environmental Science International
27(10); 901~906; October 2018

pISSN: 1225-4517 eISSN: 2287-3503
https://doi.org/10.5322/JESI.2018.27.10.901

ORIGINAL ARTICLE

A Molecular Dynamics Study of the Interaction of Oxygen Molecules with a Water Droplet

Matthew Stanley Ambrosia*

Department of Environmental Administration, Catholic University of Pusan, Busan 46252, Korea

Abstract

Water and oxygen are two of the most essential molecules for many species on earth. Their unique properties have been studied in many areas of science. In this study, the interaction of water and oxygen molecules was observed at the nano-scale. Using molecular dynamics, a water droplet with 30,968 water molecules was simulated. Then, 501 oxygen molecules were introduced into the domain. A few oxygen molecules were attracted to the surface of the water droplet due to van der Waals forces, and some oxygen molecules actually entered the water droplet. These interactions were visualized and quantified at four temperatures ranging from 280 to 370 K. It was found that at high temperatures, there was a higher possibility of the oxygen molecules penetrating the water droplet than that at lower temperatures. However, at lower temperatures, oxygen molecules were more likely to be found interacting at the surface of the water droplet than at high temperatures.

Key words : Molecular dynamics, Oxygen, Water, Temperature, Dissolution, Surface

1. Introduction

Water is not only important for life itself but also for countless processes in various industries. The interaction of oxygen with water is especially essential to biological processes, medical science, and purification processes (Marco et al., 1997; Babcock, 1999; Molinari et al., 2002). Dissolved air flotation (DAF) has been used for over a century and is a possible solution for wastewater purification (Sulman et al., 1905). DAF is a cleaning process that is used to extract particles or oils from water. This kind of water treatment uses high pressure to dissolve air and then suddenly release it in a tank of contaminated water at atmospheric pressure. Bubbles form and adhere to the contaminants in the water. After they rise to the surface of the water, the bubbles and contaminants can be skimmed off and removed. This process has been studied and applied to several areas.

Research continues in many areas concerning DAF systems. The clarification of drinking water and waste water treatment plants were the main focus of DAF in the twentieth century (Edzwald, 2010). Research continues in the domestic wastewater treatment field as pressurized aeration and DAF were integrated in a bioreactor (Zhang et al., 2014).

Received 12 October, 2018; **Revised** 23 October, 2018;
Accepted 25 October, 2018
***Corresponding author**: Matthew Stanley Ambrosia, Department of Environmental Administration, Catholic University of Pusan, Busan 46252, Korea
Phone : +82-51-510-0634
E-mail : ambrosia@cup.ac.kr

However, DAF is also used in mining and mineral processing. Micro-bubbles are used to aid the removal of contaminants from wastewater used in mining as well as the recovery of mineral particle (Rodrigues and Rubio, 2007). Not only solid particles but also oil droplet removal can be achieved with DAF. Various factors play a role in the efficiency of the extraction of oil droplets such as the purity of the water, concentration of the oil, pressure, temperature, concentration of chemical additives, and type of oil (Zouboulis and Avranas, 2000; Radzuan et al., 2016). DAF has also been studied as a desalinization pretreatment for organic matter removal. In 2016, the impacts of pH and coagulant dose on organic matter removal were recorded, and it was found that DAF would be complementary to a bio-filtration system (Shutova et al., 2016).

Experimental studies have dominated this field, but the area of computer simulation is growing and will be cheaper, easier for data collection, and require less time to produce quality results as computer technology expands. Two-phase simulations have been a challenge in the past, but new methods are being explored to simulate bubbles in DAF tanks (Chen et al., 2016; Rodrigues and Bettega, 2018).

Molecular Dynamics (MD) has also gained attention as computer processing power has boosted. MD is the simulation of molecules at the nano-scale and at nano-time-frames. A deeper understanding of molecular behaviors has been gained in the areas of material science, molecular biology, and chemical physics (Ambrosia et al., 2014; Bernardi et al., 2015; Ambrosia, 2017; Ambrosia and Ha, 2018). MD can also be applied to DAF-related issues. Recently, oxygen molecules were placed inside a nano-sized water droplet and were observed as they escaped the droplet at different temperatures (Lee and Ambrosia, 2016). However, further studies are needed to understand the phenomenon of air dissolution and bubble formation at the nano-scale.

Understanding the interaction of oxygen and water surfaces is crucial to design more efficient devices for these applications and others. In this study, the interaction of oxygen molecules with a water droplet at the nano-scale was investigated and visualized at different temperatures, using MD simulations.

2. Materials and methods

MD Simulations were applied to model a water droplet at the nano-scale along with oxygen molecules. The program called NAMD was employed to simulate the molecules' movement in this study, using a time step of 2.0 fs, and by adding up the individual forces on each molecule and applying Newton's equation of motion with a velocity Verlet algorithm (Phillips et al., 2005). Bonded potentials such as atomic bonds and angles between atoms in molecules, as well as non-bonded potentials such as van der Waals and electrostatic potentials, were considered in these calculations. The van der Waals potentials were calculated using the Lennard-Jones equation:

$$U_{LJ} = 4\epsilon_{ij}\left[\left(\frac{R_{\min}}{r_{ij}}\right)^{12} - \left(\frac{R_{\min}}{r_{ij}}\right)^{6}\right] \quad (1)$$

where U_{LJ} is the Lennard-Jones potential, ϵ_{ij} is the characteristic energy, $R_{\min}$ is the van der Waals radius, and r_{ij} is the distance between molecules *i* and *j*. The van der Waals potential decays quickly as the distance from the atom increases, and hence, it was not calculated beyond a cutoff distance of 12 Å. The Ewald method was employed for long-range electrostatic potentials. The temperature, number of atoms in the domain, as well as the volume were held constant to maintain the NVT ensemble. The velocities of the molecules were scaled to sustain the temperature for each case. The simulations comprised 501 oxygen molecules and a water droplet consisting

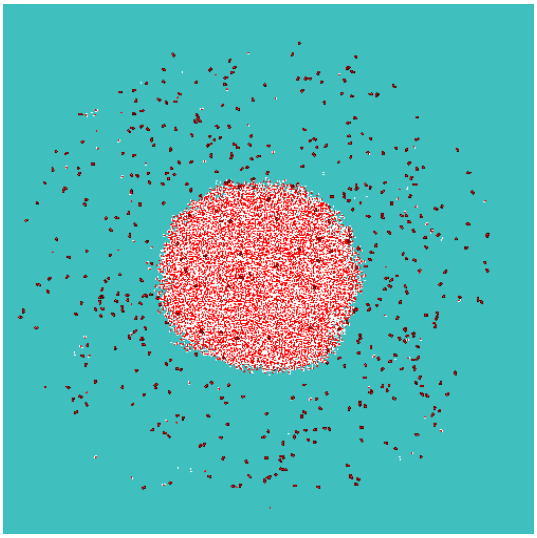

Fig. 1. The spherical computational domain with a diameter of 300 Å, containing a nano-sized water droplet with 30,968 water molecules, and the surrounding 501 oxygen molecules.

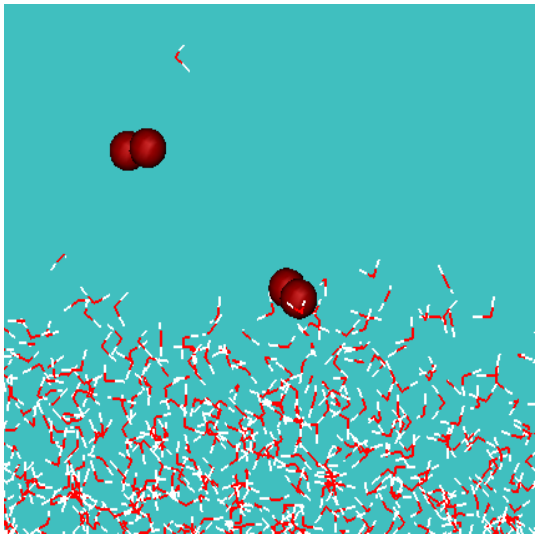

Fig. 2. A Close-up view of oxygen molecules interacting with the water surface (oxygen molecules have been enlarged for visualization).

of 30,968 transferable intermolecular potential, with 3 points (TIP3P) water molecules. TIP3P-type water molecules have two +0.417 e hydrogen atoms and one -0.834 e oxygen atom. The equilibrium angle between the atoms was set to 104.52, and we used Lennard-Jones parameters of R_{min} = 3.15061 Å and ε = 0.152 kcal/mol. The same Lennard-Jones parameter of R_{min} = 2.99 Å, which was used by Zambrano et al. (2014), was used in this study.

Firstly, a box containing the 30,968 TIP3P water molecules was modelled and simulated until the water molecules formed a spherical droplet. Then, the simulation was stopped, and the 501 oxygen molecules were inserted into the void near the water droplet. Simulations were started and run again for a period of 9 ns at 4 different temperatures of 280, 310, 340, and 370 K. The locations of the oxygen molecules were observed and recorded every 0.5 ns. Spherical boundary conditions were set to restrict the oxygen molecules from leaving the domain. The radius of this boundary was 150 Å.

3. Results and discussion

The analysis of the interaction of the oxygen molecules with the water droplet began after 1.0 ns, when the oxygen molecules completely surrounded the water droplet. Fig. 1 shows the water droplet at 1 ns. The oxygen molecules have completely surrounded the water droplet and have begun to interact with the water surface. Data was recorded from this point in time. Fig. 2 shows a close view of the interaction of the oxygen molecules with the water molecules at the surface of the water droplet. Three groups of oxygen molecules were observed. The first group entered the water droplet. The second group was within 3.5 Å from the water droplet molecules. This is the distance at which hydrogen bonds are expected to occur (Soper and Phillips, 1986). The third group was within 5 Å of the water droplet molecules.

On average, more oxygen molecules were observed in the water droplet at higher temperatures.

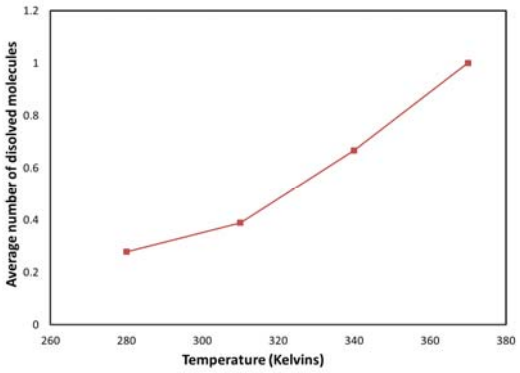

Fig. 3. Average number of dissolved oxygen molecules at different temperatures.

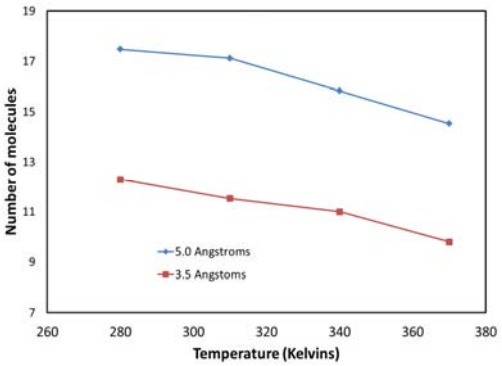

Fig. 4. The number of molecules at a distance of 3.5 and 5.0 Å from the water droplet averaged over 10 ns.

At 370 K, an oxygen molecule was 3.6 times more likely to penetrate the water droplet than at a temperature of 280 K as seen in Fig. 3, whereas it was only 2.4 times more likely at 340 K and 1.4 times more likely at 310 K. The linear relation seen in Fig. 3 is predicted by Henry's law, which states that the amount of dissolved gas is proportional to the pressure of that gas. Since the domain size remains fixed, as the temperature increases, the pressure increases proportionally, and the number of dissolved molecules also increases linearly. Henry's Law is used extensively when designing and analyzing various DAF systems. (Pouet and Grasmick, 1995; Wiley et al., 2009; Lee and Ahn, 2014) At higher temperatures, the water molecules of the water droplet have more kinetic energy, which causes them to separate more than at lower temperatures. This allows a less-defined droplet edge and a larger space between the water molecules, which makes it easier for the oxygen molecules to penetrate the water droplet. In addition, the oxygen molecules also have more kinetic energy at higher temperatures, which helps them penetrate and move between the water molecules of the water droplet.

However, it was found that, in general, there were more water molecules near the surface of the water droplet at lower temperatures than at higher temperatures. At a temperature of 280 K, an average of 12.29 molecules were found within 3.5 Å of the water droplet surface. That number steadily decreased to 11.53, 11.00, and 9.8 as the temperature increased to 310, 340, and 370 K, respectively. In addition, the average number of molecules within 5 Å of the water droplet surface decreased similarly from 17.47 molecules at 280 K to 14.53 at 370 K as seen in Fig. 4. At lower temperatures, molecules have lower velocities. Therefore, molecules are more likely to stick together as the kinetic energy is overcome by the van der Waals potential attracting the molecules in proximity.

Fig. 5 shows the number of molecules at various distances within 16 Å of a representative oxygen molecule as it moves toward and dissolves into the water droplet. Van der Waals interactions die down quickly as the distance between the molecules increases, and the van der Waals potential is 0.0 beyond the cutoff distance of 12 Å. Each timestep is 0.005 ns and timestep A is at 5.790 ns of the simulation. Since hydrogen bonds are said to be formed at 3.5 Å, the molecules are considered to be in contact when the distance separating them is within 4 Å. At timestep A, the closest water molecule

is 10 Å from the oxygen molecule. At the next timestep B, the oxygen molecule contacts the closest oxygen molecule as they are separated by 4 Å. Although the oxygen molecule at timestep B is in contact with a water molecule at the edge of the droplet, it is still not dissolved by the water and is only at the water surface, as signified by the few water molecules in proximity to the oxygen molecule. As time progresses to timestep H, the oxygen molecules are increasingly surrounded by water molecules, as the oxygen molecule moves deeper into the water droplet.

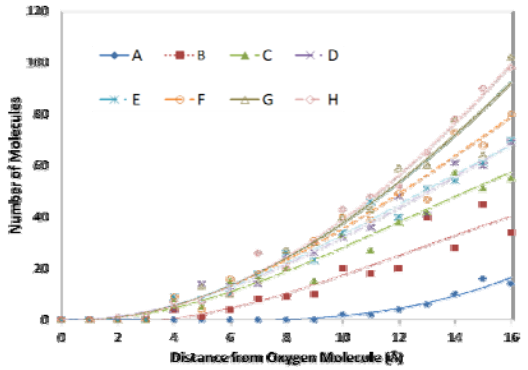

Fig. 5. Number of water molecules at various distances from an oxygen molecule as it moves into the water droplet. The times of each step are as follows: A = 5.790 ns, B = 5.795 ns, C = 5.800 ns, D = 5.805 ns, E = 5.810 ns, F = 5.815 ns, H = 5.820 ns, and I = 5.825 ns.

4. Conclusions

A nano-sized water droplet was surrounded with 501 oxygen molecules, and the oxygen-water interaction was observed for various temperatures. Oxygen molecules interacted differently with the surface of the water droplet, according to the temperature. At high temperatures water molecules were more likely to penetrate the water droplet than at lower temperatures. Oxygen molecules have more kinetic energy at higher temperatures, which helps them penetrate and move between the water molecules of the water droplet. However at lower temperatures oxygen molecules were more likely to be found interacting at the surface of the water droplet. At lower temperatures the van der Waals force is more likely to overcome the kinetic energy of a moving oxygen molecule and keep it attached to the water droplet surface. It was observed that as an oxygen molecule came into contact with and penetrated the water droplet, the oxygen molecule and water molecules maintained a distance of 2 to 4 Å. This study gives more insight into how temperature affects oxygen dissolution into water, at the nano-scale. As the understanding of this phenomenon increases, DAF systems could be designed to more easily facilitate the dissolution process of air into water.

Acknowledgements

This study was made possible thanks to the 2016 research funding from the Catholic University of Pusan.

REFERENCES

Ambrosia, M. S., Ha, M. Y., Balachandar, S., 2014, Dynamic hydrophobicity on flat and pillared graphite surfaces with different pillar surface fractions, J Mech Sci Technol, 28(2), 669-677.

Ambrosia, M. S., 2017, A Study of a nano-sized water droplet's transition from a flat surface to a pillared surface, J Mech Sci Technol, 31(2), 807-812.

Ambrosia, M. S., Ha, M. Y., 2018, A molecular dynamics study of Wenzel state water droplets on anisotropic surfaces, Computers & Fluids, 163, 1-6.

Babcock, G. T., 1999, How oxygen is activated and reduced in respiration, PNAS, 96(23), 12971-12973.

Bernardi, R. C., Melo, M. C., Schulten, K., 2015, Enhanced sampling techniques in molecular dynamics simulations of biological systems, Biochimica et Biophysica Acta (BBA) - General Subjects, 1850(5), 872-877.

Chen, A., Wang, Z., Yang, J., 2016, Influence of bubble size on the fluid dynamic behavior of a DAF tank: a 3D numerical investigation, Colloids and Surfaces A: Physicochemical and Engineering Aspects, 495, 200-207.

Edzwald, J. K., 2010, Dissolved air flotation and me, Water Research, 44(7), 2077-2106.

Lee, C. H., Ahn, K. H., 2014, Comparison of Dissolved Air and Micro-Bubble Concentration by a Micro -Bubble Generating Pump, Journal of Environmental Science International, 23(11), 1835-1842.

Lee, C. H., Ambrosia, M. S., 2016, Release of Oxygen from a Nano-sized Water Droplet Observed using Molecular Dynamics. Journal of Environmental Science International, 25(7), 927-935.

Marco, A., Esplugas, S., Saum, G., 1997, How and why combine chemical and biological processes for wastewater treatment, Water Science and Technology, 35(4), 321-327.

Molinari, R., Palmisano, L., Drioli, E., Schiavello, M., 2002, Studies on various reactor configurations for coupling photocatalysis and membrane processes in water purification, Journal of Membrane Science, 206(1 – 2), 399-415.

Phillips, J. C., Braun, R., Wang, W., Gumbart, J., Tajkhorshid, E., Villa, E., Schulten, K. 2005, Scalable molecular dynamics with NAMD, Journal of computational chemistry, 26(16), 1781-1802.

Pouet, M. F., Grasmick, A., 1995, Urban wastewater treatment by electrocoagulation and flotation, Water science and technology, 31(3-4), 275-283.

Radzuan, M. A., Belope, M. A. B., Thorpe, R. B., 2016, Removal of fine oil droplets from oil-in-water mixtures by dissolved air flotation, Chemical Engineering Research and Design, 115(A), 19-33.

Rodrigues, J. P., Béttega, R., 2018, Evaluation of multiphase CFD models for Dissolved Air Flotation (DAF) process, Colloids and Surfaces A: Physicochemical and Engineering Aspects, 539, 116-123.

Rodrigues, R. T., Rubio, J., 2007, DAF - dissolved air flotation: Potential applications in the mining and mineral processing industry, International Journal of Mineral Processing, 82(1), 1-13.

Shutova, Y., Karna, B. L., Hambly, A. C., Lau, B., Henderson, R. K., Le-Clech, P., 2016, Enhancing organic matter removal in desalination pretreatment systems by application of dissolved air flotation, Desalination, 383, 12-21.

Soper, A. K., Phillips, M. G., 1986, A New determination of the structure of water at 25 C, Chemical Physics, 107(1), 47-60.

Sulman, H. L., Picard, H. F. K., Ballot, J., 1905, Ore concentration, US Patent, No. 835120.

Wiley, P. E., Brenneman, K. J., Jacobson, A. E., 2009, Improved algal harvesting using suspended air flotation, Water Environment Research, 81(7), 702-708.

Zambrano, H. A., Walther, J. H., Jaffe, R.L., 2014, Molecular dynamics simulations of water on a hydrophilic silica surface at high air pressures, Journal of Molecular Liquids, 198, 107-113.

Zhang, Q., Liu, S., Yang, C., Chen, F., Lu, S., 2014, Bioreactor consisting of pressurized aeration and dissolved air flotation for domestic wastewater treatment, Separation and Purification Technology, 138, 186-190.

Zouboulis, A. I., Avranas, A., 2000, Treatment of oil-in-water emulsions by coagulation and dissolved -air flotation, Colloids and Surfaces A: Physicochemical and Engineering Aspects, 172(1-3), 153-161.